HYPERVELOCITY IMPACT TESTING OF NON-METALLIC MATERIALS

William P. Schonberg
Department of Mechanical Engineering
University of Alabama in Huntsville
Huntsville, Alabama 35899

ABSTRACT

The design of a spacecraft for a long-duration mission must take into account the possibility of high-speed impacts by meteoroids and orbiting space debris and the effects of such impacts on the spacecraft structure. With the use of many different kinds of materials and their proliferation in spacecraft applications, it has become necessary to evaluate their durability and their response to such high-speed projectile impact loadings. The analyses performed in this study indicate that the extent of damage in composite, ceramic, lexan, and glass structural systems can be written as functions of the geometric and material properties of the projectile/structure system. A comparative analysis of impact damage in composite and ceramic specimens and in geometrically similar aluminum specimens is performed to determine the advantages and disadvantages of employing certain composite and ceramic materials in the design of structural wall systems for long-duration spacecraft. A similar analysis of the damage in single panel lexan and multi-plane glass windows shows that glass window systems are rather resilent under hypervelocity impact loadings.

INTRODUCTION

All large spacecraft with a mission duration of more than a few days are susceptible to impacts by meteoroids and pieces of orbiting space debris. These impacts occur at extremely high speeds and can damage the flight-critical systems of a spacecraft, which can in turn lead to catastrophic failure of the spacecraft. To date, twenty-six impact craters have been found on Space Shuttle Orbiter windows[1]. While it is not precisely known how many of these are due to orbital debris impacts, the susceptibility of spacecraft windows to high-speed impacts is clearly evident. Therefore, the design of spacecrafts for long-duration missions must take into account the possibility of such impacts and their effects on the spacecraft structure and on all of its exposed components.

In order to successfully design a spacecraft for a mission into the meteoroid and space debris environment, it is necessary to be able to characterize the response of a variety of structural materials under such high speed impact loadings. Structural walls for crew compartments and spacecraft modules have traditionally consisted of a bumper plate that is placed at a small distance away from the main pressure wall of the compartment or module. This concept was first proposed by Whipple[2] and has been studied extensively in the last two decades as a means of reducing the penetration threat of hypervelocity projectiles (see, e.g. Refs. 3-10). However, in the majority of these investigations, the bumper and structural wall were typically made from metallic materials, such as aluminum or steel. With the advent of many new composite and ceramic materials and their proliferation in aircraft applications, it has become necessary to evaluate their potential for use in long-duration space and aerospace structural systems. In addition, with the installation of windows for viewing as well as scientific purposes in spacecraft such as the Space Shuttle Orbiters and the Space Station Freedom, it has become necessary to study the effect of exposing window materials to the particulate component of the space environment and to evaluate their degradation as a result of such an exposure.

One aspect of materials evaluation for use in space and aerospace structural systems is the analysis of their response to hypervelocity impact loadings. Unfortunately, information on hypervelocity impact of composite, ceramic, and window materials is scarce because work in this area has just begun[11-14]. This paper presents a summary of results of a recent investigation into the response of lexan, glass, composite panels, and ceramic panels under hypervelocity projectile impact loadings. Test results for dual-wall specimens employing three different fiber-reinforced composite materials and one ceramic material are reviewed qualitatively and quantitatively. Impact damage is characterized according to the extent of penetration, crater, and spall damage in the structural system. The damage in the composite and ceramic material specimens is also compared to the damage in geometrically similar aluminum specimens caused by hypervelocity projectiles with similar impact energies. This comparative analysis, together with the overall composite and ceramic system impact response analysis, is used to determine the advantages and disadvantages of employing composite and ceramic materials in structural wall systems for long-duration spacecraft. Two window materials of different hardness were considered in this study: lexan and glass. Several layers of lexan were glued together to form single-panel Lexgard window test specimens. The glass window test specimens consisted of three panes separated by small distances. The impact damage to the Lexgard specimens is characterized according to the extent of surface damage, the extent of internal delamination, and the area of rear-side spall damage. The impact damage in the glass specimens is characterized according to the nature of the damage to each pane in the glass window system.

The hypervelocity impact testing of the dual-wall structural systems was performed at the Space Debris Simulation Facility of the Materials and Processes Laboratory at the NASA/Marshall Space Flight Center. The facility consists of a two-stage light gas gun capable of launching 12.7 mm projectiles at velocities of 2 to 8 km/sec[15]. Projectile velocity measurements were accomplished via pulsed X-ray, laser diode detectors, and a Hall photographic station.

The conditions of the impact tests were chosen to simulate space debris impact of lightweight space structures as closely as possible, and still remain within the realm of experimental feasibility. Kessler, et.al.[16] state that the average mass density for pieces of orbital debris less than 10 mm in diameter is approximately 2.8 gm/cm^3, which is approximately the same as that of aluminum. Although it is anticipated that the shape of the impacting projectile will affect the formation and spread of secondary debris particles[17], spherical projectiles were used in the test program to maintain repeatability and consistency. Thus, the testing was conducted with solid spherical 1100 aluminum projectiles with diameters ranging from 3.175 mm to 9.525 mm. The impact velocities ranged from 3.43 to 7.40 km/sec.

HYPERVELOCITY IMPACT TESTING: DUAL-WALL STRUCTURES

In each test of a dual-wall structure, a projectile of diameter d and velocity V impacted a bumper plate of thickness t_s along a trajectory perpendicular to the plane of the bumper plate (see Figure 1). The projectile shattered upon impact and formed a hole of diameter D in the bumper plate. Secondary projectile and bumper plate debris fragments created during the impact were sprayed upon a pressure wall plate of thickness t_w located a distance S behind the bumper plate. These secondary debris impacts created an area of damage A_d on the pressure wall plate; the angle γ is the cone angle of the secondary debris fragment cloud and represents the spread of the debris fragments. Occasionally, the impacts of the secondary debris fragments resulted in the creation of spall fragments ejected from the rear side of the pressure wall plate. In these instances, the total spalled area on the rear surface is denoted by A_s.

A total of 24 aluminum, 12 composite, and 3 ceramic dual-wall structural systems were used to study and evaluate the penetration resistance of dual-wall systems with composite and ceramic bumpers. In the composite systems, the bumper plates were made of a fiber reinforced composite material while the pressure wall plates were made of 2219-T87 aluminum. The composite materials used as bumper plates were Kevlar 49 and IM6/3501-6 graphite/epoxy. In the ceramic systems, the bumper plates were made of 3 layers of 0.635 mm thick alumina (Al_2O_3) fastened together with Crest 7450 adhesive; the pressure wall plates were made of 2219-T87 aluminum. In the aluminum systems, the bumper and the pressure wall plates were made of 6061-T6 and 2219-T87 aluminum, respectively. The thicknesses of the aluminum bumper plates were chosen so that they would have approximately the *same areal density as the* composite and ceramic material plates, that is, for example,

$$t_{s',alum} = (\rho_{comp}/\rho_{alum})t_{s,comp} \qquad (1)$$

The mechanical properties and the laminae lay-up of the composite and ceramic material bumper plates are given in Tables 1 and 2, respectively; test parameters are given in Tables 3 and 4. The results of the hypervelocity impact test firings are given in Tables 5 and 6; column entries of '----' indicate that penetration and/or spall of the pressure wall plate did not occur. Detailed post-test analyses of the damaged test specimens revealed many interesting features and characteristics of composite materials hypervelocity impact response.

HYPERVELOCITY IMPACT RESPONSE OF KEVLAR SYSTEMS

Bumper Plate Damage Analysis

The impact damage in the Kevlar bumper plates typically consisted of a circular hole and large areas of delamination on the front and rear surfaces of the plates. Although the edge of the hole was usually frayed, its roundness was evident nonetheless. The delamination area of the front surface extended far beyond the the vicinity of the hole and was approximately twice as large as the delamination area of the rear surface. On both surfaces, the delamination was generally restricted to the outer layers, with the peeling in the direction of the surface laminate fibers. These observations are similar to those made in a previous study of the hypervelocity impact response of thick graphite/epoxy panels[11].

Pressure Wall Plate Damage Analysis

In Tables 7 and 8, penetration characteristics are summarized for test shots grouped according to both geometric and impact energy similarity. Table 7 shows results for impact energies below 2,000 joules (the 'low impact energy regime') while Table 8 shows results for energies greater than 10,000 joules (the 'high impact energy regime'). A penetration function for both, the Kevlar systems in the low and high energy regimes and the corresponding aluminum systems is shown in Figure 2. Using Tables 7,8 and the detailed penetration data in Tables 5,6, a comparison of penetration response characteristics was performed.

In the low impact energy regime, the pressure wall plate damage areas of the Kevlar systems were highly concentrated and consisted of either a single hole (a penetrating impact) or a single crater (a non-penetrating impact). The damage areas in similar aluminum systems were more widespread and contained numerous small holes and/or craters. Among the high energy impacts, for a 101.6 mm stand-off distance, penetration of the pressure wall plates occurred in the Kevlar as well as in the aluminum systems. The damage areas on the pressure wall plates of both structural systems were observed to be similar in size. However, when the wall spacing was increased to 152.4 mm, the Kevlar systems were penetrated while the corresponding aluminum systems were not. Furthermore, at this stand-off distance, pressure wall plate damage areas in the aluminum systems were *significantly larger* than those in the Kevlar systems. The relative magnitudes of the damage areas are also evident in Tables 5 and 6 where the secondary debris cloud cone angles in the aluminum system impacts are seen to be much larger than those in the corresponding Kevlar system impacts.

These differences in response characteristics between the aluminum and Kevlar systems indicate that aluminum bumpers are generally more effective in spreading out the secondary debris that is created by the initial projectile impact on the bumper plate, especially for impact energies above 10,000 joules. The concentration of the debris

clouds and the resultant small damage areas on the pressure wall plates in the Kevlar systems can be explained in part by a mismatch in shock impedance between the Kevlar bumper plates and the aluminum projectiles[18]. In the Kevlar systems, the shock waves in the projectile and the bumper plate created by the initial impact interacted in a manner that prevented the complete break-up of the projectile. As a result, the dispersion of the secondary projectile and bumper plate fragments also decreased. An increased probability of pressure wall plate penetration also resulted from the increased concentration of the secondary debris fragment clouds.

It is interesting to note that the reverse sides of the pressure wall plates of the Kevlar systems did not exhibit any spall at either stand-off distance, while those of the aluminum systems exhibited significant spalling at both stand-off distances. A spall function for the aluminum systems considered in this investigation is presented in Figure 3. This increased tendency for spall in the aluminum specimens is a direct consequence of the wider areal distribution of the impulse delivered by the secondary debris fragment cloud. The impulse delivered to the pressure wall plate in the Kevlar systems is more concentrated and therefore serves to penetrate the plate rather than cause spall.

HYPERVELOCITY IMPACT OF GRAPHITE/EPOXY SYSTEMS

To determine if there would be a difference in resistance to pressure wall plate penetration between dual-wall specimens with bumper plates made of Kevlar 49, aluminum 6061-T6, and graphite/epoxy, two high energy impact tests were conducted with IM6/3501-6 graphite/epoxy as the bumper plate material. A summary of the resulting penetration and spall characteristics for the graphite/epoxy and corresponding aluminum tests is presented in Table 9.

An examination of the damaged graphite/epoxy bumper plates revealed that, unlike the delamination in the Kevlar bumper plates, the impact-induced delamination on the front and rear surfaces of the graphite/epoxy plates were not very extensive. The delamination was primarily restricted to the outer layers of both surfaces and were in the general direction of the outer laminate fibers. The holes in the graphite/epoxy bumper plates were also more clearly defined than those in the Kevlar plate impacts.

The damage areas on the pressure wall plates of the graphite/epoxy systems were more widespread diffuse than those of the Kevlar systems. Although the pressure wall plates in the graphite/epoxy systems were still penetrated by the secondary debris fragments, the penetrations consisted of several small holes or craters rather than a single large hole or crater as in the Kevlar systems. Additionally, even though pressure wall plate penetration occurred in both the graphite/epoxy and the corresponding aluminum systems, the equivalent hole diameters of the penetrated pressure wall plates of the graphite/epoxy systems were significantly larger than those in the corresponding aluminum systems. Thus, the penetrations in the graphite/epoxy systems were more 'critical' than those in similar aluminum systems. Had these been on-orbit impacts, the larger penetrated areas in the graphite/epoxy systems would have allowed air to escape from a pressurized module at a higher rate than would the penetrations in the corresponding aluminum systems.

It is also noted that the pressure wall plates in the aluminum systems also exhibited significant rear side spall whereas the pressure wall plates of the graphite/epoxy systems did not. As discussed previously, this response characteristic of aluminum dual-wall systems is a serious matter and deserves further investigation.

HYPERVELOCITY IMPACT OF ALUMINA SYSTEMS

Three high energy impact tests were conducted with three-ply alumina bumper plates to determine if there would be a difference in resistance to pressure wall plate penetration between dual-wall specimens with alumina bumper plate and dual-wall specimens with aluminum 6061-T6 bumper plates. A summary of the resulting penetration and spall characteristics for the alumina and corresponding aluminum tests is presented in Table 10. It is noted that although the pressure wall plate thickness in the aluminum tests 228C,D are greater than those of the alumina tests, the total areal densities of the alumina systems and the aluminum systems in tests 228C,D are within 2.5% of each other.

An examination of the alumina bumper plate holes revealed many irregularities in their size and shape. Although all three alumina test shots were similar in impact energy, the hole in one alumina bumper plate was round (140A), while the holes in the other two (140B,C) were jagged. This indicates that multi-ply alumina bumper plates have a tendency to fracture and tear near the site of impact as well as melt or fragment.

The damage areas on the pressure wall plates of the alumina systems were similar in magnitude to those of the aluminum systems. However, the equivalent hole diameters of the penetrated pressure wall plates of the alumina systems were significantly larger than those in the corresponding aluminum systems. Thus, in a manner similar to the Kevlar and graphite/epoxy system penetrations, the penetrations in the alumina systems were more 'critical' than those in corresponding aluminum systems. It is also noted that the pressure wall plates in both the alumina and the aluminum systems exhibited rear side spall whereas the pressure wall plates of the Kevlar and graphite/epoxy systems did not. As discussed previously, the tendency of aluminum dual-wall systems to exhibit rear side spall is a serious matter and is in need of further investigation.

HYPERVELOCITY IMPACT TESTING: WINDOW MATERIALS

A total of 21 single-pane Lexgard specimens and 5 triple-pane glass specimens were used to study and evaluate the hypervelocity impact response of window materials. The Lexgard specimens were made from several 23cmx23cm Lexgard sheets of varying thicknesses glued together (Figures 4a,b). The glass specimens consisted of three 15cmx15 cm panes separated by varying stand-off distances (Figure 5). In the glass specimens, the outer and inner panes were made from annealed soda lime and

tempered Herculite II glass, respectively, while some middle panes were made from annealed soda lime glass and others from tempered Herculite II glass.

The mechanical properties of the window materials are given in Table 11; test parameters and configuration geometries for each window type are given in Tables 12,13,14. The results of the hypervelocity impact test firings are given in Tables 15, 16 for the Lexgard and glass specimens, respectively. Column entries of '----' in Table 15 indicate that penetration and/or spall of the Lexgard specimen did not occur. Detailed analyses of the damaged test specimens revealed many interesting features and response characteristics of window materials under hypervelocity projectile impact loadings.

HYPERVELOCITY IMPACT RESPONSE OF LEXGARD

Qualitative Damage Analysis

Two different window constructions were used to evaluate the response of Lexgard windows to hypervelocity projectile impact. One consisted of a 12.7 mm layer of Lexgard sandwiched in between two 3.175 mm Lexgard layers for a total specimen thickness t_w=19.05 mm (Figure 4a). The other contained an additional interior 12.7 mm layer for a total specimen thickness t_w=31.75 mm (Figure 4b). In each test, a projectile of diameter d and velocity V impacted a Lexgard window specimen along a trajectory perpendicular to the plane of the window (Figures 4a,b). The projectile shattered upon impact and created a series of shock waves that created an internal area of damage. This internal damage area was typically a circular area of delamination between the Lexgard layers. In some instances, front and rear surface petalling, as well as rear surface spall, resulted from shock wave interaction at the interface between a thin surface layer and a thick interior layer. Occasionally, penetration of the window specimen occurred as well. In these cases, the material surrounding the hole was melted and torn through the thickness of the specimen.

A summary of the damage to each of the Lexgard specimens can be found in Table 15 where D is the diameter of the hole in the specimen if penetration occured, A_d is the area of the internal damage region, and A_s is the area of rear surface spall if spall occured. Penetration functions for normal impact of both specimen types are shown in Figure 6 based on the penetration data in Table 15; a spall function for the normal impact of the thin Lexgard panels is shown in Figure 7. These curves can be used to determine if penetration or rear-surface spall will occur as a result of a particular high velocity impact. It is noted that the curves in Figures 6,7 are lines of demarcation between areas of penetration, no penetration and spall, no spall for the parameters indicated.

While rear surface spall occured frequently in the impact of the thin Lexgard specimens, it is interesting to note that rear surface spall did not occur in any of the thick specimens. Impact of the thick specimens resulted in either rear surface petalling without spall or in a 'ballooning' of the rear surface, also without spall. Additionally, the rear surface remained undamaged when a thick Lexgard specimen was impacted by the smaller projectiles; impact by the larger projectiles resulted in significant delamination between the two thick interior layers. Oblique impacts penetrated the thin specimens but not the thick specimens. At trajectory obliquities of 45^o and 65^o, the thin specimens were penetrated by 7.95 mm projectiles. However, the thick specimens were not penetrated at either trajectory obliquity, even though the projectile diameter was increased to 9.525 mm. Significant front and rear surface petalling and large areas of internal delamination were also observed in Lexgard specimens impacted by large obliquely incident projectiles.

HYPERVELOCITY IMPACT OF GLASS SYSTEMS

Two different systems were used to study the response of triple-pane glass windows to hypervelocity impact. The essential differences between the two systems were the thickness of the outer panes and the stand-off distance between the outer and middle panes (the 'outer stand-off distance'). In one triple-pane system, the outer pane thickness was 6.4 mm and the outer stand-off distance was 12.7 mm. In the other, the outer pane was 16 mm thick and the distance between the outer and middle pane was 50.8 mm. In both systems, the thicknesses of the middle and inner panes were 16 mm each; the spacing between the middle and inner panes was 12.7 mm. A summary of the resulting damage to each pane in each test is presented in Table 16. For the purposes of this investigation, a glass window specimen was considered to be penetrated if the inner pane was cracked or shattered. A shattered pane is defined as a pane that disintegrates into smaller pieces upon impact. A cracked pane has numerous fractures, but remains intact after impact. A qualitative analysis of the damage revealed many interesting features and characteristics of multi-pane window systems under hypervelocity impact.

The hypervelocity impact response of the triple-pane glass specimens was significantly different from that of the Lexgard test specimens. The damage in the glass panes was much more extensive due to their brittleness and low tensile strength. This allowed the shock-related stresses to overwhelm the material strengths for a longer period of time in the glass specimens than in the Lexgard test specimens [13]. In four of the glass tests, the outer pane was completely shattered and disintegrated. The thinner outer panes in Tests 18-1 and 18-2 were shattered into hundreds of pieces ranging from approximately 0.1 cm to 3 cm in diameter; the thicker outer panes in Tests 18-3 and 18-4 were shattered into several large chunks ranging from about 3.5 cm to 7.5 cm in diameter. In the fifth test, the outer pane was laminated and, as such, did not disintegrate upon impact. However, it was penetrated and sustained relatively large areas of spallation on both front and back surfaces. The middle panes in the specimens with the thick outer panes and the larger outer stand-off distance sustained no serious damage. The middle panes in the specimens with thinner outer panes and smaller outer stand-off distance were either cracked or shattered. The cracked middle panes contained numerous overlapping radial and concentric ring fractures. Their appearance strongly resembled that of a thick glass block subjected to a hypervelocity projectile impact[12].

The inner panes sustained no damage regardless of the thickness of the outer pane.

A more detailed examination of the damage sustained by each pane in the triple-pane glass window systems revealed that the systems with laminated panes faired better overall than did those systems without laminated panes. For example, in Test 18-2, the middle pane was laminated while in Test 18-1 it was not. Accordingly, the middle pane in Test 18-1 cracked in half while the middle pane in Test 18-2 merely sustained some cracks on the front surface and was not penetrated. Furthermore, lamination of the outer pane in Test 18-5 prevented its complete disintegration whereas the otherwise identical outer panes in Tests 18-1 and 18-2 were completely shattered under similar impacts.

From these results, it can be seen that both triple-pane glass window systems can withstand normal impacts of 3.175 mm diameter aluminum particles travelling at speeds of up to 6.6 km/sec. If such systems were used for spacecraft windows, it is unlikely that a pressure leak would occur due to an on-orbit impact of similar magnitude. If such an impact were to occur on a window system containing a thin outer pane placed at a small distance away from the middle pane, only the inner pane would be left to maintain the pressure seal. If the glass window system were to have a thin laminated outer pane or a thick outer pane placed at a relatively large distance from the middle plane, the middle pane would most likely remain undamaged and two window panes would be left to maintain the pressure seal. However, an on-orbit impact of a triple-pane glass window system with a thick outer pane would create large chunks of secondary debris which could subsequently be more damaging than the smaller secondary debris pieces created by the impact of a triple-pane window system with a thin outer pane. Lamination of both the outer and middle panes would reduce the potential for the creation of any glass debris fragments. In any case, the window would be rendered useless for viewing and scientific purposes and would necessitate the replacement of at least one pane of the window system.

SUMMARY AND CONCLUSIONS

Based on the observations made in the preceding sections, it is concluded that thin Kevlar 49, IM6/3501-6 graphite/epoxy, and alumina panels offer no advantage over equivalent aluminum 6061-T6 panels in reducing the penetration threat of hypervelocity projectiles. However, it must be noted that significant pressure wall plate spalling was observed in the alumina and the aluminum systems while no spalling was observed in either the Kevlar or the graphite/epoxy systems. It is becoming increasingly apparent that, because of the high speeds with which spall fragments can travel, impact-induced spall can be as deleterious to mission success and crew safety as an actual penetration. Naturally, the major difference between a spall event and a penetration event is the lack of a pressure leak in a spall event. However, the lethality of the high-speed spall fragments must not be overlooked.

An investigation of the hypervelocity impact response of spacecraft window materials has revealed many interesting features and response characteristics. Multi-layer Lexgard windows were found to sustain high levels of internal, penetration, and rear side spall damage as a result of normal and oblique hypervelocity impacts. The tendency of the Lexgard window panels to spall as a result of a hypervelocity impact is an area of major concern. Because of the high speeds with which spall fragments can travel, impact-induced spall can be as deleterious to mission success and crew safety as an actual penetration. The lethality of the high-speed spall fragments must not be overlooked.

Triple-pane glass window systems were found to be rather resilient under hypervelocity projectile impact loadings and did not sustain any penetration or spall damage of the inner-most window pane. Increasing the thickness of the outer pane served to reduce the number of fragments that formed when it shattered under impact; increasing the outer stand-off distance resulted in a significant decrease in the damage sustained by the middle window pane. Furthermore, it was found that laminating the outer and middle window panes prevented them from disintegrating upon impact. This is highly desireable in order that, in the event of an on-orbit glass window impact, the orbital environment does not become further contaminated by hundreds of glass debris fragments.

ACKNOWLEDGMENTS

The author is grateful for support from the NASA/Marshall Space Flight Center under contract NAS8-36955/D016. The author would also like to acknowledge the assistance of Mssrs. Kent Darzi and Russ Lakin during the data acquisition phase of this investigation.

REFERENCES

1. K. Edelstein, Orbiter Windshield Impact Testing and Analysis Meeting, NASA/Johnson Space Center, July 11, 1989.

2. E.L. Whipple, "Meteorites and Space Travel", Astron. Journal, Vol. 52, p. 137, 1947.

3. W.P. Schonberg, and R.A. Taylor, "Penetration and Ricochet Phenomena in Oblique Hypervelocity Impact", AIAA Journal, Vol. 27, pp. 639-646, 1989.

4. P.J. D'Anna, "A Combined System Concept for Control of the Meteoroid Hazard to Space Vehicles", J. Spacecraft, Vol. 2, pp. 33-37, 1965.

5. C.J. Maiden, J.W. Gehring, and A.R. McMillan, Investigation of Fundamental Mechanism of Damage to Thin Targets by Hypervelocity Projectiles, GM-DRL-TR-63-225, General Motors Defense Research Laboratory, Santa Barbara, California, 1963.

6. C.J. Maiden, and A.R. McMillan, "An Investigation of the Protection Afforded a Spacecraft by a Thin Shield", AIAA Journal, Vol. 2, pp. 1992-1998, 1964.

7. R.R. Wallace, J.R. Vinson, and M. Kornhauser, "Effects of Hypervelocity Particles on Shielded Structures", ARS Journal, pp. 1231-1237, 1962.

8. W.P. Schonberg, "Hypervelocity Impact Pene-

tration Phenomena in Aluminum Space Structures", J. Aero. Engng., Vol. 5, in press, 1990.

9. C.R. Nysmith, "An Experimental Impact Investigation of Aluminum Double-Sheet Structures", Proceedings of the AIAA Hypervelocity Impact Conference, AIAA Paper No. 69-375, 1969.

10. W.P. Schonberg, "Characterizing the Damage Potential of Ricochet Damage Debris Due to an Oblique Hypervelocity Impact", Proceedings of the Thirtieth AIAA Structures, Structural Dynamics, and Materials Conference, AIAA Paper No. 89-1410, 1989.

11. C.H. Yew and R.B. Kendrick, "A Study of Damage in Composite Panels Produced by Hypervelocity Impact", Int. J. Impact Engng., Vol. 5, pp. 729-738, 1987.

12. R.E. Flaherty, "Impact Characteristics in Fused Silica", Proceedings of the AIAA Hypervelocity Impact Conference, AIAA Paper No. 69-367, 1969.

13. B.G. Cour-Palais, "Hypervelocity Impact in Metals, Glass, and Composites", Int. J. Impact Engng., Vol. 5, pp. 221-237, 1987.

14. B.G. Cour-Palais, "Hypervelocity Impact Investigations and Meteoroid Shielding Experience Related to Apollo and Skylab", Orbital Debris, NASA CP 2360, 1982, pp. 247-75.

15. R.A. Taylor, "A Space Debris Simulation Facility for Spacecraft Materials Evaluation", SAMPE Quarterly, Vol. 18, pp. 28-34, 1987.

16. D.J. Kessler, R.C. Reynolds, and P.D. Anz-Meador, Orbital Debris Environment for Spacecraft Designed to Operate in Low Earth Orbit, NASA TM-100471, Houston, Texas, 1989.

17. R.H. Morrison, A Preliminary Investigation of Projectile Shape Effects in the Hypervelocity Impact of a Double Sheet Structure, NASA TN D-6944, Washington, D.C., 1972.

18. A.R. Coronado, M.N. Gibbins, M.A. Wright, and P.H. Stern, Space Station Integrated Wall Design and Penetration Damage Control, D180-30550-1, Boeing Aerospace Co., Seattle, Washington, 1987.

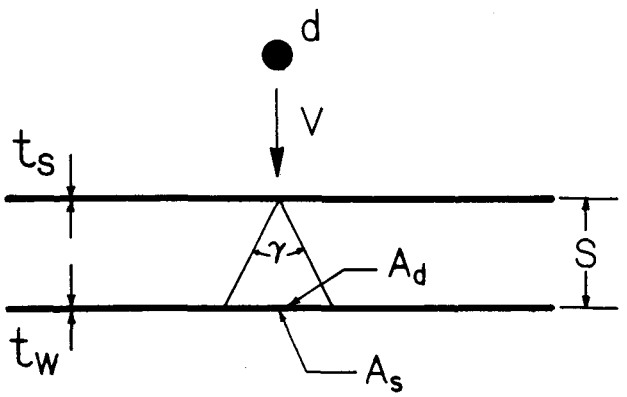

Fig. 1 Test Configuration: Dual-Wall Structure

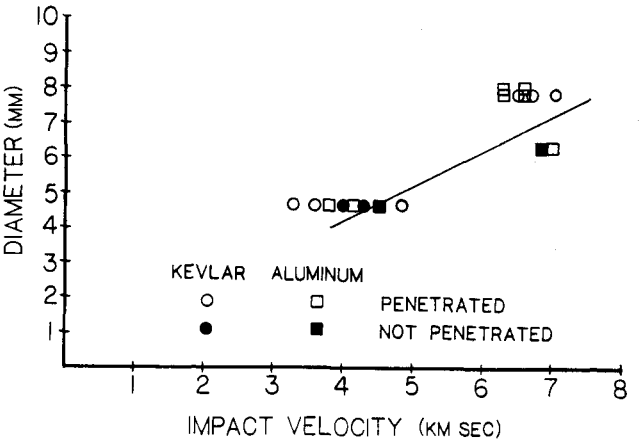

Fig. 2 Penetration Function for Kevlar (t_s=3.8 mm) and Alum. (t_s=1.6 mm) Dual-Wall Structures (t_w=3.175 mm, S=101.6 mm)

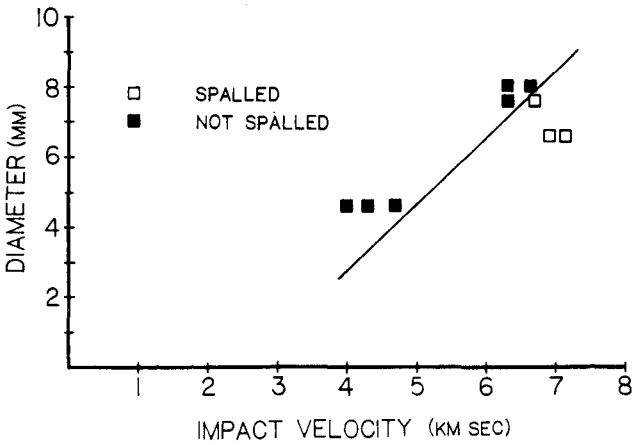

Fig. 3 Spall Function for Aluminum Dual-Wall Structures (t_s=1.6 mm, t_w=3.175 mm, S=101.6 mm)

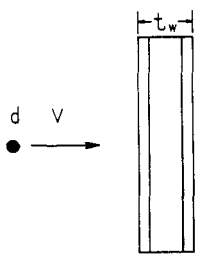

Fig. 4a Thin Lexgard Window Test Specimen

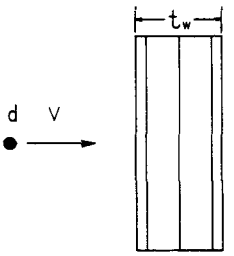

Fig. 4b Thick Lexgard Window Test Specimen

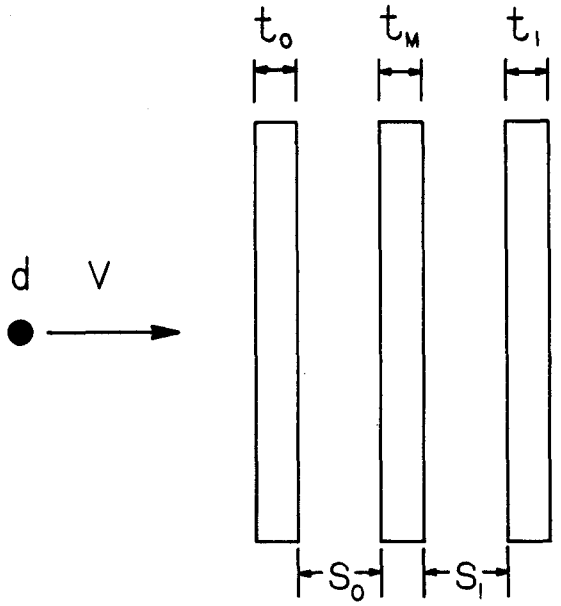

Fig. 5 Triple-Pane Glass Window Test Specimen

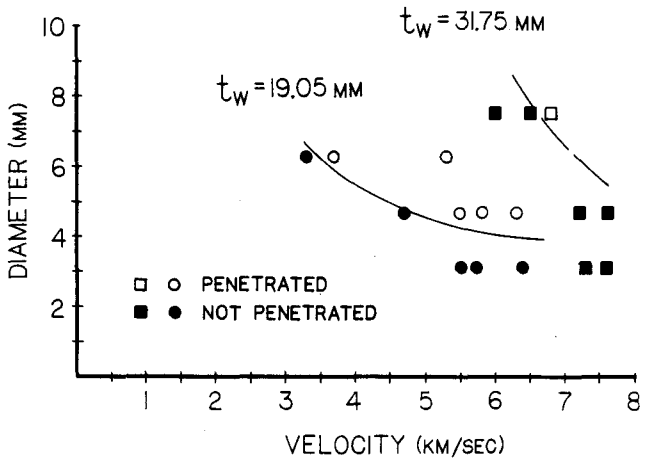

Fig. 6 Penetration Functions for Lexgard Windows

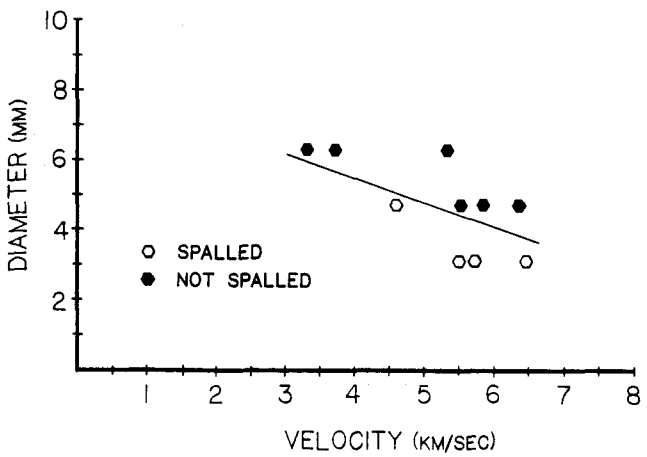

Fig. 7 Spall Function for Thin Lexgard Window

		Kevlar49	IM6/3501-6	Alumina
E	($x10^9$ N/m^2)	----	----	379.2
ν		----	----	0.317
E_1	($x10^9$ N/m^2)	76.0	203.0	----
E_2	($x10^9$ N/m^2)	5.5	11.0	----
G_{12}	($x10^9$ N/m^2)	2.3	8.3	----
ν_{12}		0.340	0.320	----
ν_{21}		0.025	0.017	----
ρ	(kg/m^3)	1340	1541	3900

Table 1 Unidirectional Ply Properties of Kevlar49 (67% fiber vol.), IM6/3501-6 Graphite/ Epoxy (63% fiber vol.), and Alumina [courtesy of NASA/MSFC and MMA]

Panel ID ID No.	Material	No. of Plies	t_s (mm)	Lamina Lay-up
C1	Kevlar 49	12	2.032	$[0,\pm60,\overline{+}60,0]_s$
C2	Kevlar 49	18	2.921	$(0,\pm60,\overline{+}60,0)_3$
C3	Kevlar 49	24	3.810	$[(0,\pm60,\overline{+}60,0)_2]_s$
C4	Graph./Epoxy	24	3.810	$[(0,\pm60,\overline{+}60,0)_2]_s$
C5	Alumina	3	1.905	----

Table 2 Geometric Properties of Composite and Ceramic Bumper Plates

Test No.	Bumper ID No.	V (km/s)	d (mm)	t_s (mm)	t_w (mm)	S (mm)
			Kevlar 49			
103	C1	4.62	4.75	2.032	3.175	101.6
103A	C3	3.52	4.75	3.810	3.175	101.6
103B	C3	3.43	4.75	3.810	3.175	101.6
103C	C3	3.84	4.75	3.810	3.175	101.6
1031	C3	4.24	4.75	3.810	3.175	101.6
104	C3	6.72	7.62	3.810	3.175	101.6
104A	C3	6.65	7.62	3.810	3.175	101.6
104B	C3	7.01	7.62	3.810	3.175	101.6
1221	C2	7.15	7.62	2.921	3.175	152.4
1222	C2	7.40	7.62	2.921	3.175	152.4
			IM6/3501-6 Graphite/Epoxy			
177A	C4	6.91	6.35	3.810	3.175	101.6
177B	C4	7.38	6.35	3.810	3.175	101.6
			Alumina			
140A	C5	6.37	6.35	1.905	3.175	101.6
140B	C5	7.23	6.35	1.905	3.175	101.6
140C	C5	6.85	6.35	1.905	3.175	101.6

Table 3 Test Parameters for Composite and Ceramic Systems

Test No.	V (km/s)	d (mm)	t_s (mm)	t_w (mm)	S (mm)
P05	6.90	6.35	1.600	3.175	101.6
P06A	6.95	6.35	1.600	3.175	101.6
P16E	6.78	7.62	1.600	3.175	152.4
P16G	7.18	7.62	1.600	3.175	152.4
P20B	6.98	7.62	1.600	3.175	152.4
P20C	6.63	7.62	1.600	3.175	152.4
P21	6.63	7.62	1.600	3.175	101.6
P21A	6.47	7.62	1.600	3.175	101.6
P27	4.53	4.75	1.600	3.175	101.6
P27A	3.87	4.75	1.600	3.175	101.6
P27B	4.15	4.75	1.600	3.175	101.6
P33	7.21	6.35	1.016	3.175	101.6
P34	6.80	6.35	1.600	2.540	101.6
101	3.09	4.75	2.032	3.175	101.6
101A	3.96	4.75	2.032	3.175	101.6
101B	4.27	4.75	2.032	3.175	101.6
107	6.80	8.89	2.032	4.445	101.6
107A	6.74	8.89	2.032	5.080	101.6
107B	6.82	8.89	2.032	5.715	101.6
109B	3.61	4.75	2.032	3.175	101.6
228C	6.96	6.35	0.813	4.775	101.6
228D	6.95	6.35	0.813	4.775	101.6
EH3A	6.64	7.95	1.600	3.175	101.6
EH6C	6.58	7.95	1.600	3.175	101.6

Table 4 Test Parameters for Aluminum Systems

Test No.	D (mm)	γ (deg)	A_d (cm^2)	d_h (mm)	A_s (cm^2)
			Kevlar 49		
103	9.271	37.9	31.68	13.538	----
103A	9.677	34.1	30.39	8.103	----
103B	9.423	30.7	24.52	8.103	----
103C	9.271	26.7	26.71	----	----
1031	9.093	43.6	51.87	----	----
104	20.193	56.5	139.68	48.387	----
104A	19.685	64.0	126.64	50.063	----
104B	19.050	61.0	145.68	46.660	----
1221	19.558	40.8	102.58	54.458	----
1222	20.193	43.1	114.32	61.874	----
			IM6/3501-6 Graphite/Epoxy		
177A	15.596	49.4	81.03	11.075	----
177B	15.191	55.4	85.16	13.716	----
			Alumina		
140A	22.301	45.6	57.72	7.645	0.619
140B	33.096	57.3	97.21	----	----
140C	35.712	53.1	81.07	7.010	0.832

Table 5 Hypervelocity Impact Test Results for Composite and Ceramic Systems

Test No.	D (mm)	γ (deg)	A_d (cm^2)	d_h (mm)	A_s (cm^2)
P05	14.224	55.9	91.55	4.699	0.19
P06A	14.529	64.0	126.71	----	4.65
P16E	15.748	53.1	182.39	23.368	12.65
P16G	16.510	60.5	248.39	----	2.88
P20B	15.875	56.8	214.06	----	5.08
P20C	15.240	56.9	214.06	2.166	6.37
P21	15.875	63.9	126.64	28.804	5.29
P21A	14.300	58.1	102.58	33.782	----
P27	10.668	40.9	45.61	----	----
P27A	8.636	29.0	21.74	4.445	----
P27B	10.033	34.6	31.68	3.048	----
P33	13.005	64.0	126.64	crack	3.34
P34	14.122	64.0	153.29	10.363	2.68
101	10.135	28.1	20.25	6.655	----
101A	9.398	31.3	25.61	4.347	----
101B	14.224	52.8	81.03	----	----
107	19.050	66.5	139.61	15.434	12.13
107A	18.288	69.1	154.97	9.018	15.48
107B	19.050	66.5	139.68	crack	13.68
109B	10.160	44.2	62.06	----	----
228C	11.024	34.7	31.68	----	9.88
228D	11.201	33.4	29.16	2.642	2.86
EH3A	15.138	75.4	206.19	49.835	----
EH6C	17.475	63.7	126.64	31.979	----

Table 6 Hypervelocity Impact Test Results for Aluminum Systems

Test Number	Bumper Plate Material	Impact Energy (J)	Impact Momentum (kg-m/s)	Pressure Wall Plate	
				Penetrated?	Spalled?
103A	Kevlar	924.9	0.536	yes	no
109B	Aluminum	991.8	0.549	no	no
103B	Kevlar	895.3	0.522	yes	no
P27A	Aluminum	1139.8	0.589	yes	no
103C	Kevlar	1122.1	0.584	no	no
101A	Aluminum	1041.8	0.563	yes	no
P27B	Aluminum	1310.7	0.632	yes	no
1031	Kevlar	1368.1	0.645	no	no
101B	Aluminum	1387.5	0.650	no	no
103	Kevlar	1624.3	0.703	yes	no
P27	Aluminum	1561.7	0.689	no	no

Table 7 Penetration Comparison of Kevlar and Aluminum Systems (Impact Energy < 2,000 joules)

Stand Off Dist.	Test Number	Bumper Plate Material	Impact Energy (J)	Impact Momentum (kg-m/s)	Pressure Wall Plate	
					Penetrated?	Spalled?
101.6 mm	104B	Kevlar	15,441	4.405	yes	no
	EH6C/3A	Aluminum	15,733	4.739	yes	no
	P21	Aluminum	13,812	4.166	yes	yes
	104	Kevlar	14,274	4.236	yes	no
	104A	Kevlar	13,896	4.179	yes	no
	P21A	Aluminum	13,154	4.066	yes	no
152.4 mm	1221	Kevlar	16,064	4.493	yes	no
	P20B	Aluminum	15,309	4.386	no	yes
	P16G	Aluminum	16,199	4.512	no	yes
	1222	Kevlar	16,699	4.581	yes	no

Table 8 Penetration Comparison of Kevlar and Aluminum Systems (Impact Energy > 10,000 joules)

Test Number	Bumper Plate Material	Impact Energy (J)	Impact Momentum (kg-m/s)	Pressure Wall Plate	
				Penetrated?	Spalled?
P05	Aluminum	8657.4	2.509	yes	yes
177A	Graphite/Epoxy	8682.5	2.513	yes	no
177B	Graphite/Epoxy	9903.8	2.684	yes	no
P34	Aluminum	8408.2	2.473	yes	yes
P33	Aluminum	9452.7	2.622	crack	yes

Table 9 Penetration Comparison of Graphite/Epoxy and Aluminum Systems

Test Number	Bumper Plate Material	Impact Energy (J)	Impact Momentum (kg-m/s)	Pressure Wall Plate	
				Penetrated?	Spalled?
228C	Aluminum	8809	2.531	no	yes
228D	Aluminum	8041	2.418	yes	yes
140A	Alumina	7378	2.317	yes	yes
140B	Alumina	9505	2.629	no	no
140C	Alumina	8532	2.491	yes	yes
P05	Aluminum	8658	2.509	yes	yes
P06A	Aluminum	8783	2.528	no	yes

Table 10 Penetration Comparison of Alumina and Aluminum Systems

		Lexgard	Soda Lime Glass	Herculite II
E	($\times 10^9$ N/m^2)	2.47	70.4	75.9
ν		----	0.22	0.21
ρ	(kg/m^3)	1150	2410	2464

Table 11 Mechanical Properties of Window Materials

Test No.	V (km/s)	θ (deg)	d (mm)	t_w (mm)
123-1	5.40	0	3.175	19.05
123-2	5.80	0	3.175	19.05
123-3	6.40	0	3.175	19.05
124-1	6.30	0	4.750	19.05
124-2	5.86	0	4.750	19.05
124-3	5.50	0	4.750	19.05
124-4	4.66	0	4.750	19.05
125A	5.27	0	6.350	19.05
125B	3.78	0	6.350	19.05
125C	3.23	0	6.350	19.05
126A	7.24	0	4.750	31.75
126B	7.46	0	4.750	31.75
127A	7.16	0	6.350	31.75
127B	7.41	0	6.350	31.75
129A	6.86	0	7.620	31.75
129B	6.45	0	7.620	31.75
129C	6.00	0	7.620	31.75
171A	6.60	45	9.525	31.75
172A	6.65	65	9.525	31.75
173A	6.91	45	7.950	19.05
174A	6.94	65	7.950	19.05

Table 12 Lexgard Impact Test Parameters

Test No.	V (km/s)	d (mm)	t_o (mm)	t_m (mm)	t_i (mm)	S_o (mm)	S_i (mm)
18-1	6.50	3.175	6.4	16.0	16.0	12.7	12.7
18-1	6.33	3.175	6.4	16.0	16.0	12.7	12.7
18-3	6.50	3.175	16.0	16.0	16.0	50.8	12.7
18-4	6.63	3.175	16.0	16.0	16.0	50.8	12.7
18-5	6.50	3.175	6.4	16.0	16.0	12.7	12.7

Table 13 Glass Impact Test Parameters

Test No.	Outer Pane	Middle Pane	Inner Pane
18-1	Soda Lime	Herculite II	Herculite II
18-2	Soda Lime	Lam. Herc. II	Herculite II
18-3	Soda Lime	Soda Lime	Herculite II
18-4	Soda Lime	Lam. S.L.	Herculite II
18-5	Lam. S.L.	Lam. S.L.	Herculite II

Table 14 Glass Window Pane Materials

Test No.	D (mm)	A_d (cm^2)	A_s (cm^2)
123-1	----	24.45	2.787
123-2	----	20.26	1.510
123-3	----	33.48	0.806
124-1	7.493	64.71	----
124-2	6.299	63.29	----
124-3	5.791	49.81	----
124-4	----	59.10	1.026
125A	10.414	113. 42	----
125B	6.756	60.32	----
125C	----	51.81	----
126A	----	135.03	----
126B	----	109.42	----
127A	----	182.06	----
127B	----	188.39	----
129A	6.629	230.84	----
129B	----	159.61	----
129C	----	186.32	----
171A	----	387.93	----
172A	----	230.52	----
173A	45.7x53.3	153.29	----
174A	31.750	167.55	----

Table 15 Hypervelocity Impact Test Results for Lexgard Panels

Test No.	Outer Pane	Middle Pane	Inner Pane	Penetr.?
18-1	Shattered; ≃100 fragments 0.1 to 2.5 cm	Shattered	No Damage	No
18-2	Shattered; ≃100 fragments 0.1 to 3.2 cm	Cracked No Penetration	No Damage	No
18-3	Shattered; 19 fragments 3.5 to 7.5 cm	Minor Pitting	No Damage	No
18-4	Shattered; 6 fragments 3.5 to 5.1 cm	Minor Pitting	No Damage	No
18-5	3.25 mm hole; 4.3 cm dia. spall on both surfaces; No Disintegration	Cracked No Penetration	No Damage	No

Table 16 Hypervelocity Impact Test Results for Glass Systems